Nuclear Effects on $R = \sigma_L/\sigma_T$ in Deep-Inelastic Scattering

The HERMES Collaboration

K. Ackerstaff[5], A. Airapetian[33], N. Akopov[33], I. Akushevich[6], M. Amarian[25,28,33], E.C. Aschenauer[6,13,25], H. Avakian[10], R. Avakian[33], A. Avetissian[33], B. Bains[15], C. Baumgarten[23], M. Beckmann[12], S. Belostotski[26], J.E. Belz[29,30], Th. Benisch[8], S. Bernreuther[8], N. Bianchi[10], J. Blouw[25], H. Böttcher[6], A. Borissov[5,14], M. Bouwhuis[15], J. Brack[4], S. Brauksiepe[12], B. Braun[8,23], B. Bray[3], St. Brons[6], W. Brückner[14], A. Brüll[14], E.E.W. Bruins[20], H.J. Bulten[18,25,32], G.P. Capitani[10], P. Carter[3], P. Chumney[24], E. Cisbani[28], G.R. Court[17], P. F. Dalpiaz[9], E. De Sanctis[10], D. De Schepper[2,20], E. Devitsin[22], P.K.A. de Witt Huberts[25], P. Di Nezza[10], M. Düren[8], A. Dvoredsky[3], G. Elbakian[33], J. Ely[4], A. Fantoni[10], A. Fechtchenko[7], M. Ferstl[8], K. Fiedler[8], B.W. Filippone[3], H. Fischer[12], B. Fox[4], J. Franz[12], S. Frullani[28], M.-A. Funk[5], Y. Gärber[6], H. Gao[2,15,20], F. Garibaldi[28], G. Gavrilov[26], P. Geiger[14], V. Gharibyan[33], A. Golendukhin[5,19,23,33], G. Graw[23], O. Grebeniouk[26], P.W. Green[1,30], L.G. Greeniaus[1,30], C. Grosshauser[8], M. Guidal[25], A. Gute[8], V. Gyurjyan[10], J.P. Haas[24], W. Haeberli[18], J.-O. Hansen[2], M. Hartig[30], D. Hasch[6,10], O. Häusser†[29,30], F.H. Heinsius[12], R. Henderson[30], M. Henoch[8], R. Hertenberger[23], Y. Holler[5], R.J. Holt[15], W. Hoprich[14], H. Ihssen[5,25], M. Iodice[28], A. Izotov[26], H.E. Jackson[2], A. Jgoun[26], R. Kaiser[6,29,30], E. Kinney[4], M. Kirsch[8], A. Kisselev[26], P. Kitching[1], H. Kobayashi[31], N. Koch[19], K. Königsmann[12], M. Kolstein[25], H. Kolster[23], V. Korotkov[6], W. Korsch[3,16], V. Kozlov[22], L.H. Kramer[11,20], V.G. Krivokhijine[7], M. Kurisuno[31], G. Kyle[24], W. Lachnit[8], P. Lenisa[9], W. Lorenzon[21], N.C.R. Makins[2,15], F.K. Martens[1], J.W. Martin[20], F. Masoli[9], A. Mateos[20], M. McAndrew[17], K. McIlhany[3,20], R.D. McKeown[3], F. Meissner[6], F. Menden[12,30], A. Metz[23], N. Meyners[5] O. Miklouk ho[26], C.A. Miller[1,30], M.A. Miller[15], R. Milner[20], A. Most[15,21], V. Muccifora[10], R. Mussa[9], A. Nagaitsev[7], Yu. Naryshkin[26], A.M. Nathan[15], F. Neunreither[8], J.M. Niczyporuk[15,20], W.-D. Nowak[6], M. Nupieri[10] T.G. O'Neill[2], R. Openshaw[30], J. Ouyang[30], B.R. Owen[15], V. Papavassiliou[24], S.F. Pate[20,24], M. Pitt[3], S. Potashov[22], D.H. Potterveld[2], G. Rakness[4], A. Reali[9], R. Redwine[20], A.R. Reolon[10], R. Ristinen[4], K. Rith[8], P. Rossi[10], S. Rudnitsky[21], M. Ruh[12], D. Ryckbosch[13], Y. Sakemi[31], I. Savin[7], C. Scarlett[21], A. Schäfer[27], F. Schmidt[8], H. Schmitt[12], G. Schnell[24], K.P. Schüler[5], A. Schwind[6], J. Seibert[12], T.-A. Shibata[31], K. Shibatani[31], T. Shin[20], V. Shutov[7], C. Simani[9], A. Simon[12,24], K. Sinram[5], P. Slavich[9,10], M. Spengos[5], E. Steffens[8], J. Stenger[8], J. Stewart[17], U. Stoesslein[6], M. Sutter[20], H. Tallini[17], S. Taroian[33], A. Terkulov[22], E. Thomas[10], B. Tipton[20], M. Tytgat[13], G.M. Urciuoli[28], J.F.J. van den Brand[25,32], G. van der Steenhoven[25], R. van de Vyver[13], J.J. van Hunen[25], M.C. Vetterli[29,30], V. Vikhrov[26], M.G. Vincter[1,30], J. Visser[25], E. Volk[14], W. Wander[8,20], J. Wendland[29], S.E. Williamson[15], T. Wise[18], K. Woller[5], S. Yoneyama[31], H. Zohrabian[33],

[1] *Department of Physics, University of Alberta, Edmonton, Alberta T6G 2J1, Canada*
[2] *Physics Division, Argonne National Laboratory, Argonne, Illinois 60439-4843, USA*
[3] *W.K. Kellogg Radiation Laboratory, California Institute of Technology, Pasadena, California 91125, USA*
[4] *Nuclear Physics Laboratory, University of Colorado, Boulder, Colorado 80309-0446, USA*
[5] *DESY, Deutsches Elektronen Synchrotron, 22603 Hamburg, Germany*
[6] *DESY Zeuthen, 15738 Zeuthen, Germany*
[7] *Joint Institute for Nuclear Research, 141980 Dubna, Russia*
[8] *Physikalisches Institut, Universität Erlangen-Nürnberg, 91058 Erlangen, Germany*
[9] *Istituto Nazionale di Fisica Nucleare, Sezione di Ferrara and Dipartimento di Fisica, Università di Ferrara, 44100 Ferrara, Italy*
[10] *Istituto Nazionale di Fisica Nucleare, Laboratori Nazionali di Frascati, 00044 Frascati, Italy*
[11] *Department of Physics, Florida International University, Miami, Florida 33199, USA*
[12] *Fakultät für Physik, Universität Freiburg, 79104 Freiburg, Germany*
[13] *Department of Subatomic and Radiation Physics, University of Gent, 9000 Gent, Belgium*
[14] *Max-Planck-Institut für Kernphysik, 69029 Heidelberg, Germany*
[15] *Department of Physics, University of Illinois, Urbana, Illinois 61801, USA*
[16] *Department of Physics and Astronomy, University of Kentucky, Lexington, Kentucky 40506,USA*
[17] *Physics Department, University of Liverpool, Liverpool L69 7ZE, United Kingdom*
[18] *Department of Physics, University of Wisconsin-Madison, Madison, Wisconsin 53706, USA*
[19] *Physikalisches Institut, Philipps-Universität Marburg, 35037 Marburg, Germany*
[20] *Laboratory for Nuclear Science, Massachusetts Institute of Technology, Cambridge, Massachusetts 02139, USA*
[21] *Randall Laboratory of Physics, University of Michigan, Ann Arbor, Michigan 48109-1120, USA*
[22] *Lebedev Physical Institute, 117924 Moscow, Russia*
[23] *Sektion Physik, Universität München, 85748 Garching, Germany*
[24] *Department of Physics, New Mexico State University, Las Cruces, New Mexico 88003, USA*
[25] *Nationaal Instituut voor Kernfysica en Hoge-Energiefysica (NIKHEF), 1009 DB Amsterdam, The Netherlands*

[26] *Petersburg Nuclear Physics Institute, St. Petersburg, 188350 Russia*
[27] *Institut für Theoretische Physik, Universität Regensburg, 93040 Regensburg, Germany*
[28] *Istituto Nazionale di Fisica Nucleare, Sezione Sanità and Physics Laboratory, Istituto Superiore di Sanità, 00161 Roma, Italy*
[29] *Department of Physics, Simon Fraser University, Burnaby, British Columbia V5A 1S6, Canada*
[30] *TRIUMF, Vancouver, British Columbia V6T 2A3, Canada*
[31] *Department of Physics, Tokyo Institute of Technology, Tokyo 152, Japan*
[32] *Department of Physics and Astronomy, Vrije Universiteit, 1081 HV Amsterdam, The Netherlands*
[33] *Yerevan Physics Institute, 375036, Yerevan, Armenia*

(October 18, 1999)

Cross section ratios for deep-inelastic scattering from ^{14}N and ^{3}He with respect to ^{2}H have been measured by the HERMES experiment at DESY using a 27.5 GeV positron beam. The data cover a range in the Bjorken scaling variable x between 0.013 and 0.65, while the negative squared four-momentum transfer Q^2 varies from 0.5 to 15 GeV^2. The data are compared to measurements performed by NMC, E665, and SLAC on ^{4}He and ^{12}C, and are found to be different for $x < 0.06$ and $Q^2 < 1.5$ GeV^2. The observed difference is attributed to an A-dependence of the ratio $R = \sigma_L/\sigma_T$ of longitudinal to transverse deep-inelastic scattering cross sections at low x and low Q^2.

PACS numbers: 13.60.Hb, 13.60.-r, 24.85.+p, 12.38.-t

The energy scales relevant to deep-inelastic lepton nucleon scattering (multi-GeV) greatly differ from those relevant to the atomic nucleus (multi-MeV). Hence, it came as a surprise that the structure function $F_2^N(x)$, which in the Quark-Parton Model represents the quark momentum distribution inside the nucleon, was found to depend on the mass A of the atomic nucleus [1]. This phenomenon is known as the *EMC effect* at large values of the Bjorken scaling variable x, i.e. $x > 0.1$, and as *shadowing* at lower values of x [2].

With $F_2(x)$ found to be A-dependent, it is relevant to investigate whether this dependence is the same for its longitudinal and transverse components, $F_L(x)$ and $F_1(x)$. The latter two structure functions are related to $F_2(x)$ via $F_L(x) = (1+Q^2/\nu^2)F_2(x) - 2xF_1(x)$ with Q^2 the negative of the four-momentum transfer squared q^2, ν the energy transfer, $x = Q^2/2M\nu$ and M the nucleon mass. A possible difference of the A-dependence of $F_L(x)$ and $F_1(x)$ can be investigated by measuring the ratio of longitudinal to transverse deep-inelastic scattering (DIS) cross sections $R = \sigma_L/\sigma_T = F_L(x)/2xF_1(x)$ for various nuclear targets.

Theoretically, a possible A-dependence of R has been suggested by several authors. In ref. [3] the Fermi motion of the nucleons is seen to enhance higher-twist effects, which will lead to an enhancement of $F_L(x)$ at low values of x and Q^2. It has also been argued [4] that an increase of the nuclear gluon distribution may lead to an enhancement of R. On the other hand, in ref. [5] it is suggested that nuclear shadowing might be different for the longitudinal and transverse DIS cross sections. The predicted size and (x,Q^2)-dependence of these effects are all different. However, no experimental evidence for an A-dependence of R has been found to date [6–9].

In this Letter we present data from the HERMES experiment on the cross section ratio for deep-inelastic positron scattering off nitrogen and helium-3 with respect to deuterium. These ratios are compared to similar ratios measured in deep-inelastic scattering by NMC [10], E665 [11], and SLAC [12]. The ratio of the inclusive DIS cross sections on ^{14}N (^{3}He) and ^{2}H is presented in figure 1. A significant difference between the present data and previous data is observed for $x < 0.06$. In this domain the HERMES data for both nuclei are smaller than the NMC and E665 data and the deviation increases towards smaller values of x. At high values of x the HERMES data are in agreement with the SLAC data. In the following it is shown how the difference between the NMC and HERMES measurements can be attributed to an A-dependence of R at low values of x and Q^2.

Apart from the data shown in figure 1, other data exist which show a strong reduction of σ_A/σ_D for $0.01 < x < 0.1$ and $0.05 < Q^2 < 1.5$ GeV^2 that is similar to that of the HERMES data on ^{14}N [13,14]. However, these data were never used to study a possible A-dependence of R, either because of insufficient statistics [14], or because of their limited kinematic coverage [13].

In deep-inelastic charged lepton scattering from an unpolarised target, the double-differential cross section per nucleon can be written in the one-photon exchange approximation as

$$\frac{d^2\sigma}{dxdQ^2} = \frac{4\pi\alpha^2}{Q^4}\frac{F_2(x,Q^2)}{x} \times \left[1 - y - \frac{xyM}{2E} + \frac{y^2}{2}\left(\frac{1+4M^2x^2/Q^2}{1+R(x,Q^2)}\right)\right] = \frac{\sigma_{\rm Mott}}{E'E}\frac{\pi F_2(x,Q^2)}{x\epsilon}\left[\frac{1+\epsilon R(x,Q^2)}{1+R(x,Q^2)}\right], \quad (1)$$

where $y = \nu/E$, $\sigma_{\rm Mott}$ represents the cross section for lepton scattering from a point charge, and E and E' are the initial and final lepton energy, respectively. The virtual photon polarisation parameter is given by

$$\epsilon = \frac{4(1-y) - \frac{Q^2}{E^2}}{4(1-y) + 2y^2 + \frac{Q^2}{E^2}}. \quad (2)$$

The ratio of DIS cross sections from nucleus A and deuterium D (=^{2}H) is then given by:

$$\frac{\sigma_A}{\sigma_D} = \frac{F_2^A}{F_2^D}\frac{(1+\epsilon R_A)(1+R_D)}{(1+R_A)(1+\epsilon R_D)}, \quad (3)$$

where R_A and R_D represent the ratio σ_L/σ_T for nucleus A and deuterium. For $\epsilon \to 1$ the cross section ratio equals the ratio of structure functions F_2^A/F_2^D. For smaller values of ϵ the cross section ratio is equal to F_2^A/F_2^D only if $R_A = R_D$. A difference between R_A and R_D will thus introduce an ϵ-dependence of σ_A/σ_D. Hence, measurements of σ_A/σ_D as a function of ϵ can be used to extract experimental information on R_A/R_D, if R_D is known.

The data presented in this paper were collected by the HERMES experiment at DESY using ^{1}H, ^{2}H, ^{3}He, and ^{14}N internal gas targets in the 27.5 GeV positron storage ring of HERA. The target gases were injected into a tubular open-ended storage cell inside the positron ring. The cell provides a 40 cm long target with areal densities of up to 6×10^{15} nucleons/cm^2 for ^{14}N. The luminosity was measured by detecting Bhabha-scattered target electrons in coincidence with the scattered positrons, in a pair of $NaBi(WO_4)_2$ electromagnetic calorimeters. Dead times of less than 5% were observed even at the highest luminosities of about 10^{33} nucleons/(cm^{2}s). Systematic uncertainties in the measurements of the cross section ratios were minimized by cycling among different target gases every 2 – 4 hours during part of the data taking.

In the HERMES spectrometer [15] both the scattered positrons and the produced hadrons can be detected and identified within an angular acceptance ± 170 mrad horizontally, and 40 – 140 mrad vertically. The trigger was formed from a coincidence between a pair of scintillator

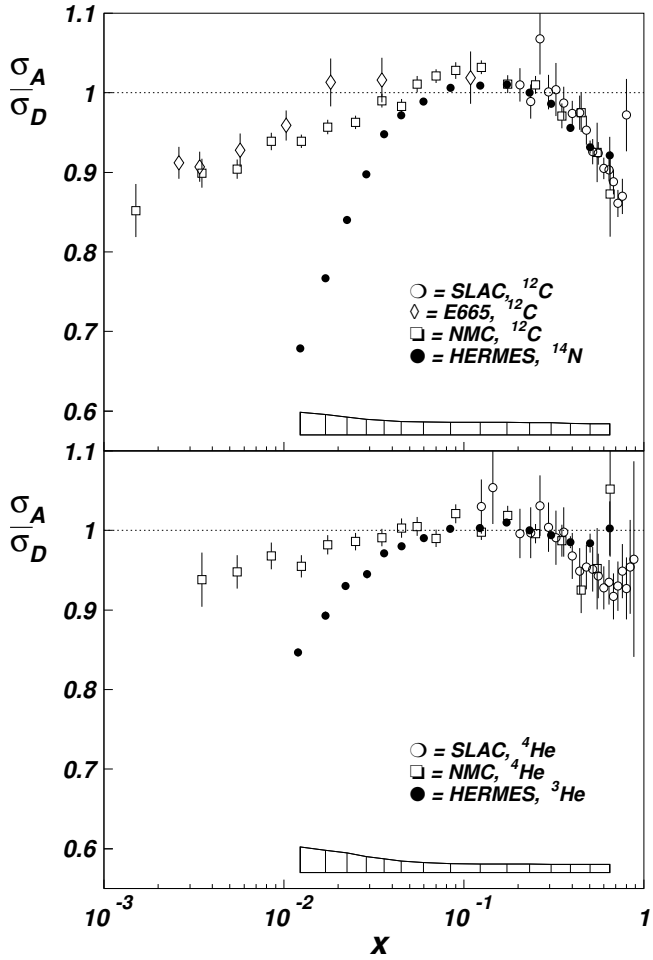

FIG. 1. Ratio of cross sections of inclusive deep-inelastic lepton scattering from nucleus A and D versus x. The error bars of the HERMES measurement represent the statistical uncertainties, the systematic uncertainty of the HERMES data is given by the error band. The error bars of the NMC, E665, and SLAC data are given by the quadratic sum of the statistical and systematic uncertainties.

hodoscope planes and a lead-glass calorimeter. The trigger required an energy of more than 3.5 GeV deposited in the calorimeter, resulting in a typical trigger rate of 100 Hz. Positron identification was accomplished using the calorimeter, the second hodoscope, which functioned as a preshower counter, a transition radiation detector, and a threshold gas Čerenkov counter. This system provided positron identification with an average efficiency of 99 % and a hadron contamination of less than 1 %.

Deep-inelastic scattering events were extracted from the data by imposing constraints on Q^2, W (the invariant mass of the photon-nucleon system), and y. For each event it was required that $Q^2 > 0.3$ GeV^2, $W > 2$ GeV and $y < 0.85$.

As the ratio σ_A/σ_D involves nuclei with different numbers of protons, radiative corrections do not cancel in the ratio. In particular, the radiative processes associated with elastic and quasi-elastic scattering are different for the two target nuclei. These radiative corrections have been computed using the methods outlined in Ref. [16]. In the cross section ratio the correction associated with elastic (i.e. coherent) scattering from the target nucleus is dominant.

Several input parameters are needed for the calculation of the radiative corrections. For the evaluation of the coherent radiative tails, the nuclear elastic form factors must be known. Parameterisations of the form factors of ^{2}H, ^{3}He, and ^{14}N were taken from the literature [17–19]. For the quasi-elastic tails, the nucleon form factor parameterisation of Gari and Krümpelmann [20] was used. The reduction of the bound nucleon cross section with respect to the free nucleon one (quasi-elastic suppression) was evaluated using the results of a calculation by Bernabeu [21] for deuterium and the non-relativistic Fermi gas model for ^{3}He and ^{14}N [22]. The evaluation of the inelastic higher order QED processes requires the knowledge of both F_2 and R over a wide range of x and Q^2. The structure function $F_2^D(x,Q^2)$ was described by a parameterisation of the NMC, SLAC, and BCDMS data [23]; for R_D the Whitlow parameterisation [24] was used. As the values of $F_2^A(x,Q^2)$ and $R_A(x,Q^2)$ are unknown for ^{3}He and ^{14}N, an iterative procedure has been used. As a starting point the nuclear structure functions $F_2^A(x,Q^2)$ were taken from phenomenological fits to the SLAC and NMC data, and $R_A(x,Q^2)$ was assumed to be equal to $R_D(x,Q^2)$. The resulting radiatively corrected values of σ_A/σ_D were used to determine F_2^A/F_2^D and R_A/R_D, which were given as input to the radiative correction code in the next step until convergence was reached. It is noted that the large difference between the NMC/E665 and HERMES values of σ_A/σ_D is already present if the NMC and SLAC parameterisations are used for $F_2(x,Q^2)$ and $R(x,Q^2)$. The iteration procedure, which converges in three steps, enlarges the difference by about 40 % (for ^{14}N) in the lowest x bins.

The size of the radiative corrections is largest in the lowest x-bin, where it amounts to 0.552, 0.461, and 0.372 for ^{2}H, ^{3}He, and ^{14}N, respectively. The systematic uncertainty in the radiative corrections was estimated by using upper and lower limits of the parameterisations, or alternative parameterisations [23–26] for all the above input parameters. The total systematic uncertainty in the cross section ratios varies from 5 % (4 %) at low x to 2 % (1 %) at high x for ^{14}N (^{3}He). It includes the normalization uncertainty of 2 % (1 %) and the uncertainty in the radiative corrections, which is dominant.

The effects originating from the finite resolution of the spectrometer and from the hadron contamination in the positron sample have been determined and found to be negligible. As a cross check of the understanding of the entire analysis chain including the radiative corrections, the cross section ratio of deuterium and hydrogen has been determined as a function of x and Q^2. The

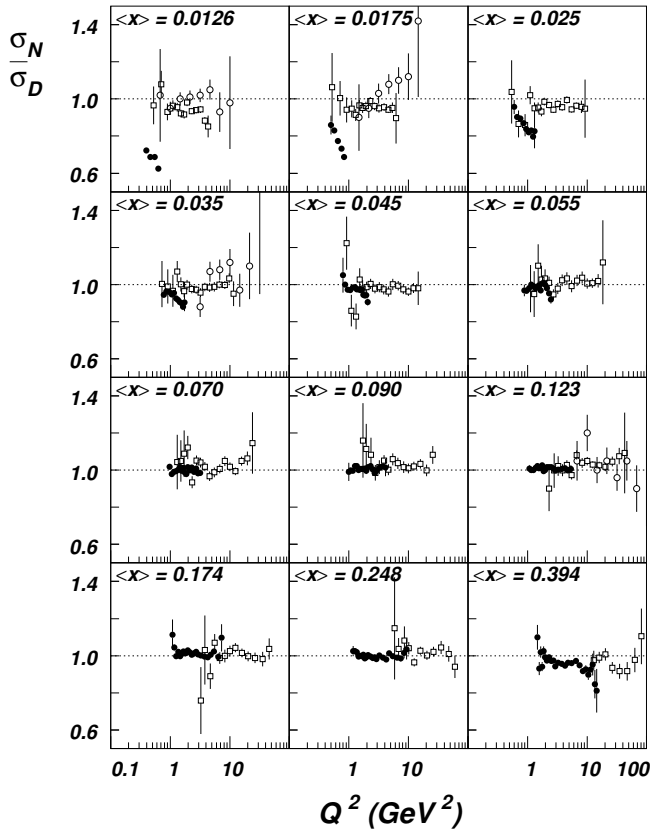

FIG. 2. Cross section ratios of inclusive deep-inelastic lepton scattering from ^{14}N to ^{2}H versus Q^2 for specific x-bins (solid circles). Also shown are the ^{12}C/^{2}H data of NMC (open squares) and E665 (open circles). Only statistical errors are shown.

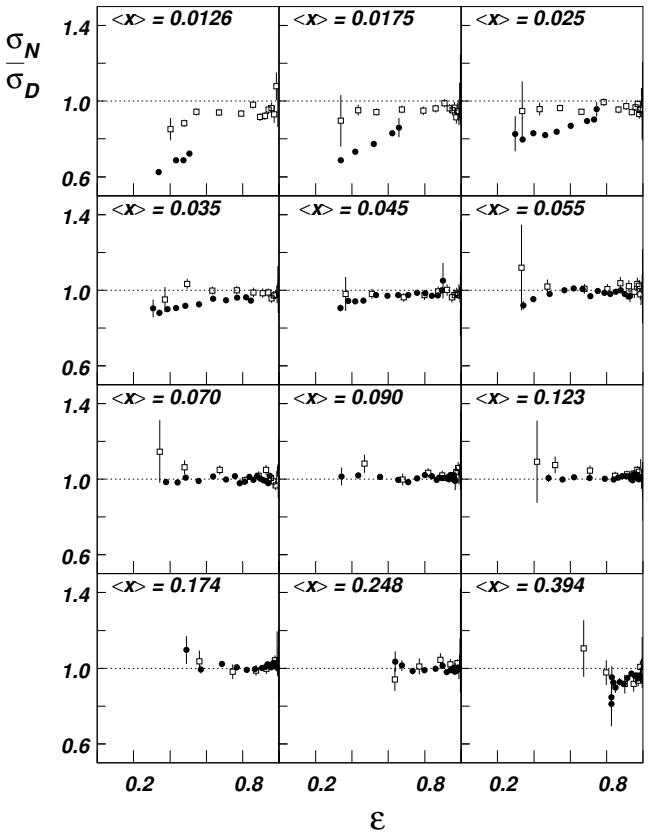

FIG. 3. Cross section ratios of inclusive deep-inelastic lepton scattering from ^{14}N to ^{2}H versus ϵ for individual x-bins (solid circles). Also shown are the ^{12}C / ^{2}H data of NMC (open squares). Note that the two data sets correspond to different Q^2 ranges. Only statistical errors are shown.

HERMES measurement [27] of σ_D/σ_p agrees within the systematic uncertainties (3 % at low x down to 1.5 % at high x) with the results from earlier experiments [28,29].

The results of the analysis [30,31] are shown in figure 1 as a function of x. It is noted that throughout the analysis the σ_{3He}/σ_D data have been corrected for the excess of protons over neutrons in ^{3}He using the measured σ_D/σ_p ratios [28]. The σ_{14N}/σ_D data are displayed in more detail in figure 2 as function of Q^2 for fixed values of x. In the first four x-bins a striking discrepancy between the HERMES and NMC data is observed. The discrepancy increases with Q^2, but at the same time the average deviation in each x bin decreases with x. Moreover, as the data show a discontinuity with respect to Q^2 for the same four lowest x-bins, it is unlikely that the discrepancy observed in figure 1 is caused by scaling violations of the ratio $F_2^A(x)/F_2^D(x)$.

As the structure function ratio F_2^A/F_2^D depends only on x and Q^2, the observed difference in the cross section ratios measured at HERMES and NMC/E665 can be explained only by an A-dependence of the ratio $R(x,Q^2)$. Therefore, in figure 3 the data have been plotted versus ϵ for fixed values of x. The ϵ-dependence of the HERMES data shows that the deviation with respect to unity decreases with increasing ϵ values. This is in accordance with the anticipated behaviour of σ_A/σ_D if R_A differs from R_D, as displayed by Eq. (3). In contrast to the HERMES data, the NMC data show no or very little ϵ-dependence. However, the two data sets shown in figure 3 at the same ϵ and average x values correspond to different Q^2 values, as can be seen by comparing the same x-bins in figures 2 and 3.

The data of the individual x-bins of figure 3 have been fitted using Eq. (3). Separate fits for the HERMES and NMC data have been performed. In these fits a parameterisation of R_D [32] has been used, while the ratios R_A/R_D and F_2^A/F_2^D have been treated as free parameters. A single value of R_A/R_D and F_2^A/F_2^D has been extracted from each x-bin in figure 3 for both the HERMES and NMC data at the average x and Q^2 values of each experiment. In this procedure it is assumed that both R_A/R_D and F_2^A/F_2^D are constant over the limited Q^2 range covered by the data in each x-bin. While the Q^2-dependence of F_2^A/F_2^D is known to be very small [33,35], the effect of a possible Q^2-dependence on the extracted values of R_A/R_D has been studied separately. Assuming

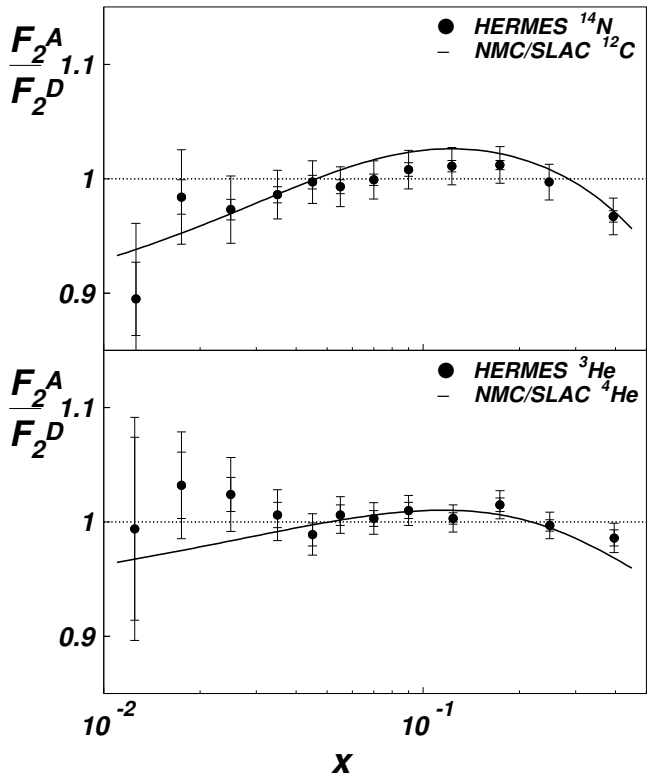

FIG. 4. The ratio of the inclusive structure functions F_2^A/F_2^D versus x as derived from the fit of the ϵ dependence of the cross section ratios. The HERMES data on ^{14}N are shown in the upper panel and those collected on ^{3}He in the lower panel. The data are compared to parameterisations of the F_2^A/F_2^D ratio for A=4 and 12, which were determined using the NMC and SLAC data [10,12]. The inner error bars include the statistical uncertainty and the correlated error in R_A/R_D. The outer error bars represent the total uncertainty including the systematic uncertainty.

a linear Q^2-dependence of R_A/R_D, it has been verified that the Q^2-range covered by each x-bin does not affect the average values of R_A/R_D derived from the fit.

The values of F_2^A/F_2^D derived from the fit of the HERMES data are displayed in figure 4 for both nitrogen and helium-3. The statistical uncertainty and the effect of the correlated error in R_A/R_D (inner error bars) are indicated separately from the total uncertainty that includes the systematic uncertainties as well (outer error bars). The data are compared to curves representing parameterisations of the F_2^A/F_2^D ratios for $A = 4$ and 12, which were determined using the NMC and SLAC data [10,12]. The data are seen to be in agreement with the parameterisations. The uncertainties on F_2^A/F_2^D are too large to observe any systematic deviation between F_2^A/F_2^D for neighbouring nuclei.

The resulting values of R_A/R_D are shown in figure 5. The error bars include the statistical uncertainty, the correlated error in F_2^A/F_2^D and the systematic uncertainty. Both the present results, which were obtained from the fits of the HERMES and NMC data shown in figure 3, and the results derived from other sources are displayed. The data are plotted at the average value of Q^2 for a given x-bin. The values of R_A/R_D derived from the HERMES data are considerably larger than unity for $x < 0.06$ and $Q^2 < 1.5$ GeV^2. The deviation from unity is smaller for ^{3}He than for ^{14}N, as one would expect for a medium dependent effect. The results of the fits of the NMC data for ^{4}He and ^{12}C, which were collected at higher average Q^2 values, are all consistent with unity. The present data for R_A/R_D are also compared to the results of previous studies of the A-dependence of R. Existing data are usually represented in terms of $\Delta R = R_A - R_D$. The published values of ΔR [32,34,35] have been converted to R_A/R_D using a parameterisation for R_D [32], and added to figure 5. All data above $Q^2 = 1.5$ GeV^2 are seen to be consistent with unity, while for $x < 0.06$ and $Q^2 < 1.5$ GeV^2 a strong Q^2-dependence is observed. It is noted that the R_A/R_D data below $x = 0.15$ can be described by an inverse power of Q^2, independent of x.

Possible mechanisms that give rise to an enhancement of R_A with respect to R_D at low Q^2 and x are constrained by the present data to not significantly change the ratio of structure functions F_2^A/F_2^D. Since F_2^A and R_A depend differently on the longitudinal and transverse DIS cross sections, the different effects of the nuclear medium on σ_L and σ_T can be distinguished. In fact, both an enhancement of the longitudinal response and a corresponding reduction of the transverse response are needed to explain the present data. Evaluated explicitly for the lowest three x-bins of the ^{14}N/^{2}H data, we find values of 2.15(40), 2.32(25), and 1.78(15) for σ_L^A/σ_L^D, and the values 0.45(4), 0.47(3), and 0.65(2) for σ_T^A/σ_T^D. These results appearing at low Q^2 and low x seem to indicate a novel large shadowing effect not contained in current theoretical models. Possible shadowing differences between σ_L and σ_T have been discussed in refs. [5,36]. The quoted enhancement of R_A with respect to R_D does not exceed 50 % [36]. However, these studies did not cover the kinematics of the present experiment. It is noted that a satisfactory description of our data should also encompass the real-photon data, which show less shadowing ($\sigma_T^A/\sigma_T^D = 0.77(5)$ for ^{12}C at $Q^2 = 0$) than the virtual-photon data at low Q^2 (see [37,13]).

The steep Q^2-dependence of the data also suggests an explanation in terms of a higher twist effect [38], i.e. strong quark-gluon correlations that are enhanced in the nuclear environment [39]. This conclusion is supported by the fact that leading twist effects are estimated to be much smaller than the observed enhancement of R_A/R_D [40,4]. The size of twist-4 effects in nuclei has been estimated by Luo, Qiu and Sterman [41] for dijet photoproduction. They find sizable enhancement factors of order 100 % that scale as $A^{1/3}$.

In order to arrive at a proper interpretation of the data presented in this paper, the quoted effects must be

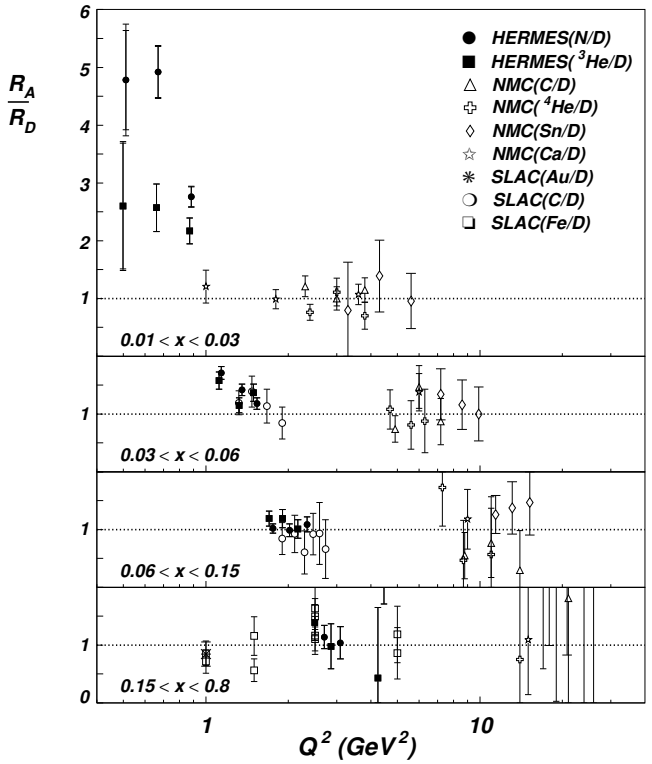

FIG. 5. The ratio R_A/R_D for nucleus A and deuterium as a function of Q^2 for four different x bins. The HERMES data on ^{14}N (^{3}He) are represented by the solid circles (squares). The open triangles (^{12}C) and crosses (^{4}He) have been derived from the NMC data using the same technique. The other SLAC [34] and NMC data [35] displayed have been derived from measurements of $\Delta R = R_A - R_D$ taking a parameterisation [32] for R_D. The inner error bars include both the statistical uncertainty and the correlated error in F_2^A/F_2^D. The outer error bars also include the systematic uncertainties.

evaluated explicitly for the conditions of our experiment. Experimentally, it is important to extend the present measurements to heavier nuclei such that the A-dependence of the effect can be determined precisely.

In summary, deep-inelastic positron scattering data on ^{2}H, ^{3}He, and ^{14}N are presented. At low values of x and Q^2, a large difference is observed between the presently measured cross section ratios σ_{3He}/σ_D and σ_{14N}/σ_D, and those reported by previous experiments at higher values of Q^2. Values for the ratio of R_A/R_D with R the ratio σ_L/σ_T of longitudinal to transverse DIS cross sections have been derived from the dependence of the data on the virtual photon polarization parameter ϵ. The data show a strong Q^2-dependence of R_A/R_D at low x and Q^2 and represent the first observation of a nuclear effect in the ratio of longitudinal to transverse photoabsorption cross sections. The uncertainty in the measurements is dominated by our estimate of the systematic uncertainty in the radiative corrections. In the absence of explicit calculations, it can be speculated that our result represents evidence for the existence of enhanced quark-gluon correlations in atomic nuclei.

ACKNOWLEDGMENTS

We gratefully acknowledge the DESY management for its support and the DESY staff and the staffs of the collaborating institutions. This work was supported by the FWO-Flanders, Belgium; the Natural Sciences and Engineering Research Council of Canada; the INTAS and TMR network contributions from the European Community; the German Bundesministerium für Bildung, Wissenschaft, Forschung und Technologie; the Deutscher Akademischer Austauschdienst (DAAD); the Italian Istituto Nazionale di Fisica Nucleare (INFN); Monbusho International Scientific Research Program, JSPS, and Toray Science Foundation of Japan; the Dutch Foundation for Fundamenteel Onderzoek der Materie (FOM); the U.K. Particle Physics and Astronomy Research Council; and the U.S. Department of Energy and National Science Foundation.

[1] J.J. Aubert et al. (EMC), Phys. Lett **B 123** (1983) 275.
[2] M. Arneodo, Phys. Rep. **240** (1994) 301.
[3] J. Milana, Phys. Rev. **C 49** (1994) 2820.
[4] T. Gousset and H.J. Pirner, Phys. Lett. **B 375** (1996) 349.
[5] N.N. Nikolaev and B.G. Zakharov, Z. Phys. **C 49** (1991) 607.
[6] P. Amaudruz et al. (NMC), Phys. Lett **B 294** (1992) 120.
[7] M. Arneodo et al. (NMC), Nucl. Phys. **B 481** (1996) 23.
[8] S. Dasu et al. (SLAC), Phys. Rev. **D 49** (1994) 5641.
[9] L. H. Tao et al. (SLAC), Z. Phys. **C 70** (1996) 387.
[10] P. Amaudruz et al. (NMC), Nucl. Phys. **B 441** (1995) 3.
[11] M.R. Adams et al. (E665), Z. Phys. **C 67** (1995) 403.
[12] J. Gomez et al., Phys. Rev. **D 49** (1994) 4348.
[13] J. Franz et al., Z. Phys. **C 10** (1981) 105; J. Bailey et al., Nucl. Phys. **B 151** (1979) 367; J. Eickmeyer et al., Phys. Rev. Lett. **36** (1976) 289; S. Stein et al, Phys. Rev. **D 12** (1975) 1884.
[14] M.S. Goodman et al., Phys. Rev. Lett. **47** (1981) 293.
[15] K. Ackerstaff et al. (HERMES), Nucl. Instr. and Meth. **A 417** (1998) 230.
[16] A.A. Akhundov, D.Yu. Bardin and N.M. Shumeiko, Sov. J. Nucl. Phys. **26** (1977) 660; D.Yu. Bardin and N.M. Shumeiko, Sov. J. Nucl. Phys. **29** (1979) 499; and A.A. Akhundov, et al., Sov. J. Nucl. Phys. **44** (1986) 988.
[17] A. Svarc and M.P. Locher, Fizika **22** (1990) 549; M.P. Locher and A. Svarc, Z. Phys. **A 338** (1991) 89.
[18] J.S. McCarthy, I. Sick and R.R. Whitney, Phys. Rev. **C 15** (1977) 1396.
[19] C.W. de Jager et al., Atom. Data and Nucl. Data Tables **14** (1974) 479.

[20] M. Gari and W. Krümpelmann, Z. Phys. **A 322** (1985) 689.
[21] J. Bernabeu, Nucl. Phys. **B 49** (1972) 186.
[22] E.J. Moniz et al., Phys. Rev. **184** (1969) 1154.
[23] M. Arneodo et al. (NMC), Phys. Lett. **B 346** (1995) 107.
[24] L.W. Whitlow et al., Phys. Lett. **B 250** (1990) 193.
[25] S. Platchkov, Nucl. Phys. **A 510** (1990) 740; P.C. Dunn et al., Phys. Rev. **C 26** (1983) 71. H. de Vries et al., Atom. Data and Nucl. Data Tables **36** (1987) 501; and R.L. Huffmann et al., Phys. Lett. **B 139** (1984) 249.
[26] H. Arenhövel, private communication (1998); D. Day, private communication (1998)
[27] A. Brüll, Proc. of the 9th Mini-Conference on 'Electromagnetic Studies of the Deuteron', Amsterdam, 1 - 2 Febr. 1996, Eds. B.L.G. Bakker, Tj. Ketel, and H. de Vries, p. 136 (1996).
[28] M. Arneodo et al. (NMC), Nucl. Phys. **B 487** (1997) 3.
[29] L.W. Whitlow et al., Phys. Lett. **B 282** (1992) 475.
[30] J.J. van Hunen, Ph.D. thesis, Utrecht University, in preparation (2000).
[31] T. Shin, Ph.D. thesis, Massachusetts Institute of Technology, in preparation (2000).
[32] K. Abe et al. (SLAC), Phys. Lett. **B 452** (1999) 194.
[33] M. Arneodo et al. (NMC), Nucl. Phys. **B 441** (1995) 12.
[34] S. Dasu et al. (SLAC), Phys. Rev. **D 49** (1994) 5641.
[35] P. Amaudruz et al. (NMC), Phys. Lett. **B 294** (1992) 120; and M. Arneodo et al. (NMC), Phys. Lett. **B 481** (1996) 23.
[36] V. Barone and M. Genovese, Proc. of the Workshop 1995/96 on 'Future Physics at HERA', Eds. G. Ingelman, A De Roeck, and R. Klanner, DESY, 1996, p. 938, hep-ph/9610206.
[37] L. Criegee et al., Nucl. Phys. **B 121** (1977) 38.
[38] R.K. Ellis, W. Furmanski and R. Petronzio, Nucl. Phys. **B 207** (1982) 1.
[39] S. Barshay and D. Rein, Z. Phys. **C 46** (1990) 215.
[40] B. Kopeliovich and M. Strikman, private communication.
[41] M. Luo, J. Qiu and G. Sterman, Phys. Rev. **D 49** (1994) 4493.